
Exact marginal prior distributions of finite Bayesian neural networks

Jacob A. Zavatone-Veth

Department of Physics
Harvard University
Cambridge, MA 02138
jzavatoneveth@g.harvard.edu

Cengiz Pehlevan

John A. Paulson School of Engineering and Applied Sciences
Harvard University
Cambridge, MA 02138
cpehlevan@seas.harvard.edu

Abstract

Bayesian neural networks are theoretically well-understood only in the infinite-width limit, where Gaussian priors over network weights yield Gaussian priors over network outputs. Recent work has suggested that finite Bayesian networks may outperform their infinite counterparts, but their non-Gaussian function space priors have been characterized only through perturbative approaches. Here, we derive exact solutions for the function space priors for individual input examples of a class of finite fully-connected feedforward Bayesian neural networks. For deep linear networks, the prior has a simple expression in terms of the Meijer G -function. The prior of a finite ReLU network is a mixture of the priors of linear networks of smaller widths, corresponding to different numbers of active units in each layer. Our results unify previous descriptions of finite network priors in terms of their tail decay and large-width behavior.

1 Introduction

Modern Bayesian neural networks (BNNs) ubiquitously employ isotropic Gaussian priors over their weights [1–22]. Despite their simplicity, these weight priors induce richly complex priors over the network’s outputs [1, 4–22]. These function space priors are well-understood only in the limit of infinite hidden layer width, in which they become Gaussian [4–8]. However, these infinite networks cannot flexibly adapt to represent the structure of data during inference, an ability that is key to the empirical successes of deep learning, Bayesian or otherwise [2, 3, 9–14, 16–20, 23, 24]. As a result, elucidating how finite-width networks differ from their infinite-width cousins is an important objective for theoretical study.

Progress towards this goal has been made through systematic study of the leading asymptotic corrections to the infinite-width prior [12, 14–17], including approaches emphasizing the physical framework of effective field theory [13, 14]. However, the applicability of these perturbative approaches to narrow networks, particularly those with extremely narrow bottleneck layers [9], remains unclear. In this paper, we present an alternative treatment of a simple class of BNNs, drawing inspiration from the study of exactly solvable models in physics [25–27]. Our primary contributions are as follows:

- We derive exact formulas for the priors over the output preactivations of finite fully-connected feedforward linear or ReLU BNNs without bias terms induced by Gaussian priors over their weights (§3). We only consider the prior for a single input example, not the joint prior over the outputs for multiple input examples, as it can capture many finite-width effects [9, 12]. Our result for the prior of a linear network is given in terms of the Meijer G -function, which is an extremely general but well-studied special function [28–32]. The prior of a ReLU network is a mixture of the priors of linear networks of narrower widths, corresponding to different numbers of active ReLUs in each layer.
- We leverage our exact formulas to provide a simple characterization of finite-width network priors (§4). The fact that the priors of finite-width networks become heavy-tailed with increasing depth and decreasing width [21, 22], as well as the asymptotic expansions for the priors at large hidden layer widths [12, 15], follow as corollaries of our main results. Moreover, we show that the perturbative finite-width corrections do not capture the heavy-tailed nature of the true prior.

To the best of our knowledge, our results constitute the first exact solutions for the priors over the outputs of finite deep BNNs. As one might expect from knowledge of even the simplest interacting systems in physics [25–27], these solutions display many intricate, non-Gaussian properties, despite the fact that they are obtained for a somewhat simplified setting.

2 Preliminaries

In this section, we define our notation and problem setting. We use subscripts to index layer-dependent quantities. We denote the standard ℓ_2 inner product of two vectors $\mathbf{a}, \mathbf{b} \in \mathbb{R}^n$ by $\mathbf{a} \cdot \mathbf{b}$. Depending on context, we use $\|\cdot\|$ to denote the ℓ_2 norm on vectors or the Frobenius norm on matrices.

We consider a fully-connected feedforward neural network $\mathbf{f} : \mathbb{R}^{n_0} \rightarrow \mathbb{R}^{n_d}$ with d layers and no bias terms, defined recursively in terms of its preactivations \mathbf{h}_ℓ as

$$\mathbf{h}_0 = \mathbf{x}, \quad (1)$$

$$\mathbf{h}_\ell = W_\ell \phi_{\ell-1}(\mathbf{h}_{\ell-1}) \quad (\ell = 1, \dots, d), \quad (2)$$

$$\mathbf{f} = \phi_d(\mathbf{h}_d), \quad (3)$$

where n_ℓ is the width of the ℓ -th layer (i.e., $\mathbf{h}_\ell \in \mathbb{R}^{n_\ell}$) and the activation functions ϕ_ℓ act elementwise [2, 3]. Without loss of generality, we take the input activation function ϕ_0 to be the identity. We consider linear and ReLU networks, with $\phi_\ell(x) = x$ or $\phi_\ell(x) = \max\{0, x\}$ for $\ell = 1, \dots, d-1$, respectively. As we focus on the output preactivations \mathbf{h}_d , we do not impose any assumptions on the output activation function ϕ_d .

We take the prior over the weight matrices to be an isotropic Gaussian distribution [1–14, 16–22], with

$$[W_\ell]_{ij} \underset{\text{i.i.d.}}{\sim} \mathcal{N}(0, \sigma_\ell^2) \quad (4)$$

for layer-dependent variances σ_ℓ^2 . Depending on how one chooses σ_ℓ —in particular, how it scales with the network width—this setup can account for most commonly-used neural network parameterizations [24]. In particular, one usually takes $\sigma_\ell^2 = \zeta_\ell^2/n_{\ell-1}$ for some width-independent ζ_ℓ^2 [2–8, 12, 24]. This weight prior induces a conditional Gaussian prior over the preactivations at the ℓ -th layer [4–8]:

$$\mathbf{h}_\ell | \mathbf{h}_{\ell-1} \sim \mathcal{N}(\mathbf{0}, \sigma_\ell^2 \|\phi_{\ell-1}(\mathbf{h}_{\ell-1})\|^2 I_{n_\ell}), \quad (5)$$

where the prior for the first hidden layer is conditioned on the input \mathbf{x} , which we henceforth assume to be non-zero. Thus, the joint prior of the preactivations at all layers of the network for a given input \mathbf{x} is of the form

$$p(\mathbf{h}_1, \dots, \mathbf{h}_d | \mathbf{x}) = p(\mathbf{h}_d | \mathbf{h}_{d-1}) p(\mathbf{h}_{d-1} | \mathbf{h}_{d-2}) \cdots p(\mathbf{h}_1 | \mathbf{x}). \quad (6)$$

To perform single-sample inference of the network outputs with a likelihood function $p_l(\mathbf{y} | \mathbf{h}_d)$ for some target output $\mathbf{y} = \mathbf{y}(\mathbf{x})$, one must compute the posterior

$$p(\mathbf{h}_d | \mathbf{x}, \mathbf{y}) = \frac{p_l(\mathbf{y} | \mathbf{h}_d, \mathbf{x}) p_d(\mathbf{h}_d | \mathbf{x})}{p(\mathbf{y} | \mathbf{x})}, \quad (7)$$

where $p(\mathbf{y} | \mathbf{x}) = \int d\mathbf{h}_d p_l(\mathbf{y} | \mathbf{h}_d, \mathbf{x}) p_d(\mathbf{h}_d | \mathbf{x})$ [1, 4–13, 18–20]. Before computing the posterior, it is therefore necessary to marginalize out the hidden layer preactivations $\mathbf{h}_1, \dots, \mathbf{h}_{d-1}$ to obtain the prior density of the output preactivation $p_d(\mathbf{h}_d | \mathbf{x})$. Moreover, in this framework, all information about the network’s inductive bias is encoded in the prior $p_d(\mathbf{h}_d | \mathbf{x})$, as the likelihood is independent of the network architecture and the prior over the weights. This marginalization has previously been studied perturbatively in limiting cases [4–9, 12, 14]; here we perform it exactly for any width.

To integrate out the hidden layer preactivations, it is convenient to work with the characteristic function $\varphi_d(\mathbf{q}_d | \mathbf{x})$ corresponding to the density $p_d(\mathbf{h}_d | \mathbf{x})$. Adopting a convention for the Fourier transform such that

$$p_d(\mathbf{h}_d | \mathbf{x}) = \int \frac{d\mathbf{q}_d}{(2\pi)^{n_d}} \exp(i\mathbf{q}_d \cdot \mathbf{h}_d) \varphi_d(\mathbf{q}_d | \mathbf{x}), \quad (8)$$

it follows from (5) that this characteristic function is given as

$$\varphi_d(\mathbf{q}_d | \mathbf{x}) = \int \prod_{\ell=1}^{d-1} \frac{d\mathbf{q}_\ell d\mathbf{h}_\ell}{(2\pi)^{n_\ell}} \exp \left(\sum_{\ell=1}^{d-1} i\mathbf{q}_\ell \cdot \mathbf{h}_\ell - \frac{1}{2} \sum_{\ell=1}^d \sigma_\ell^2 \|\mathbf{q}_\ell\|^2 \|\phi_{\ell-1}(\mathbf{h}_{\ell-1})\|^2 \right). \quad (9)$$

We immediately observe that the characteristic function is radial, i.e., $\varphi_d(\mathbf{q}_d | \mathbf{x}) = \varphi_d(\|\mathbf{q}_d\| | \mathbf{x})$. As the inverse Fourier transform of a radial function is radial [33], this implies that the preactivation prior is radial, i.e., $p_d(\mathbf{h}_d | \mathbf{x}) = p_d(\|\mathbf{h}_d\| | \mathbf{x})$. Moreover, as the prior at any given layer is separable over the neurons of that layer, we can see that $p_d(\mathbf{h}_d | \mathbf{x})$ has the property that the marginal prior distribution of some subset of k of the outputs of a network with $n_d > k$ outputs is identical to the full prior distribution of a network with k outputs. As detailed in Appendix A, these properties enable us to exploit the relationship between the Fourier transforms of radial functions and the Hankel transform, which underlies our calculational approach.

3 Exact priors of finite deep networks

Here, we present our main results for the priors of finite deep linear and ReLU networks, deferring their detailed derivations to Appendices A and B of the Supplemental Material.

3.1 Two-layer linear networks

As a warm-up, we first consider a linear network with a single hidden layer. In this case, we can easily evaluate the integral (9) to obtain the characteristic function

$$\varphi_2(\mathbf{q}_2 | \mathbf{x}) = (1 + \kappa_2^2 \|\mathbf{q}_2\|^2)^{-n_1/2}, \quad (10)$$

where we define the quantity $\kappa_2 \equiv \sigma_1 \sigma_2 \|\mathbf{x}\|$ for brevity. We can now directly evaluate the required Hankel transform to obtain the prior density (see Appendix A.1), yielding

$$p_2(\mathbf{h}_2 | \mathbf{x}) = \frac{1}{(4\pi\kappa_2^2)^{n_2/2}} \frac{2}{\Gamma(n_1/2)} \left(\frac{\|\mathbf{h}_2\|}{2\kappa_2} \right)^{(n_1-n_2)/2} K_{(n_1-n_2)/2} \left(\frac{\|\mathbf{h}_2\|}{\kappa_2} \right), \quad (11)$$

where Γ is the Euler gamma function and $K_\nu(z)$ is the modified Bessel function of the second kind of order ν [28–30].

Interestingly, we recognize this result as the distribution of the sum of $n_1/2$ independent n_2 -dimensional multivariate Laplace random variables with covariance matrix $2\kappa_2^2 I_{n_2}$ [34]. Moreover, we can see from the characteristic function (10) that we recover the expected Gaussian behavior at infinite width provided that $\kappa_2^2 \propto 1/n_1$ [4–8], as one would expect from the interpretation of this prior as a sum of i.i.d. random vectors. To our knowledge, this simple correspondence has not been previously noted in the literature, though it provides a succinct explanation of the slight heavy-tailedness of this prior distribution noted by Vladimirova et al. [21, 22]. The fact that the function space prior is heavy-tailed at finite width is a particularly important non-Gaussian feature. These results are plotted in Figure 1.

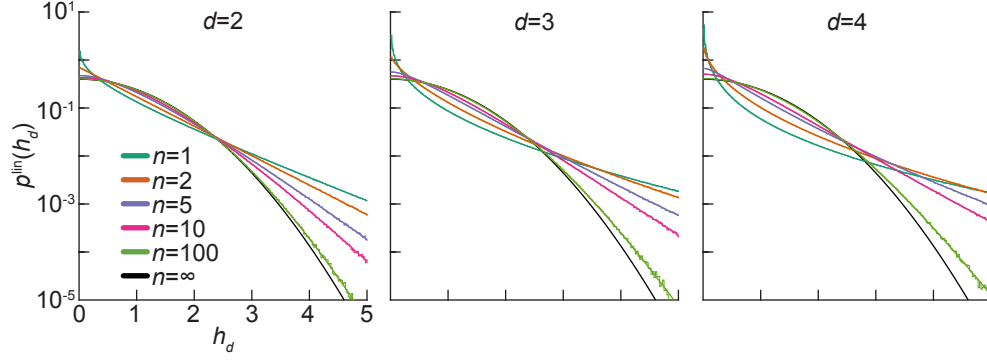


Figure 1: Priors of deep linear networks of depths $d = 2, 3$, and 4 . In each panel, the prior density is plotted only for positive values of the output preactivation h_d , as it is symmetric about zero. For each depth, all hidden layers are of the same width n , which is indicated by line color. The black line indicates the Gaussian infinite-width limit discussed in §4.3. Thick lines show the exact priors, while thin jagged lines show experimental estimates from 10^8 examples. Further details on the numerical methods used to generate these figures are provided in Appendix E.

3.2 General deep linear networks

We now consider a general deep linear network. Deferring the details of our derivation to Appendix A, we find that the characteristic function and density of the function space preactivation prior for such a network can be expressed in terms of the Meijer G -function [28, 29]. The Meijer G -function is an extremely general special function, of which most classical special functions are special cases. Despite its great generality, it is quite well-studied, and provides a powerful tool in the study of integral transforms [28–31]. Its standard definition, introduced by Erdélyi [29], is as follows: Let $0 \leq m \leq q$ and $0 \leq n \leq p$ be integers, and let a_1, \dots, a_p and b_1, \dots, b_q be real or complex parameters such that none of $a_k - b_j$ are positive integers when $1 \leq k \leq n$ and $1 \leq j \leq m$. Then, the Meijer G -function is defined via the Mellin-Barnes integral

$$G_{p,q}^{m,n} \left(z \left| \begin{matrix} a_1, \dots, a_p \\ b_1, \dots, b_q \end{matrix} \right. \right) = \frac{1}{2\pi i} \int_C ds z^s \frac{\prod_{j=1}^m \Gamma(b_j - s) \prod_{k=1}^n \Gamma(1 - a_k + s)}{\prod_{j=m+1}^q \Gamma(1 - b_j + s) \prod_{k=n+1}^p \Gamma(a_k + s)}, \quad (12)$$

where empty products are interpreted as unity and the integration path C separates the poles of $\Gamma(b_j - s)$ from those of $\Gamma(1 - a_k + s)$ [28, 29]. Expressing the density or characteristic function of a radial distribution in terms of the Meijer G -function is useful because one can then immediately read off its Mellin spectrum and absolute moments [28, 29]. Moreover, one can exploit integral identities for the Meijer G -function to compute other expectations and transformations of the density [28–31].

With this definition, the characteristic function and density of the prior of a deep linear network are given as

$$\varphi_d^{\text{lin}}(\mathbf{q}_d | \mathbf{x}) = \gamma_d G_{d-1,1}^{1,d-1} \left(2^{d-2} \kappa_d^2 \|\mathbf{q}_d\|^2 \left| \begin{matrix} 1 - n_1/2, \dots, 1 - n_{d-1}/2 \\ 0 \end{matrix} \right. \right) \quad (13)$$

and

$$p_d^{\text{lin}}(\mathbf{h}_d | \mathbf{x}) = \frac{\gamma_d}{(2^d \pi \kappa_d^2)^{n_d/2}} G_{0,d}^{d,0} \left(\frac{\|\mathbf{h}_d\|^2}{2^d \kappa_d^2} \left| \begin{matrix} - \\ 0, (n_1 - n_d)/2, \dots, (n_{d-1} - n_d)/2 \end{matrix} \right. \right), \quad (14)$$

respectively, where we define the quantities

$$\kappa_d \equiv \sigma_1 \cdots \sigma_d \|\mathbf{x}\| \quad \text{and} \quad \gamma_d \equiv \prod_{\ell=1}^{d-1} \frac{1}{\Gamma(n_\ell/2)} \quad (15)$$

for brevity. Here, the horizontal dash in the upper row of arguments to $G_{0,d}^{d,0}$ indicates the absence of ‘upper’ arguments to the G -function, denoted by a_1, \dots, a_p in (12), because $p = 0$. For $d = 2$,

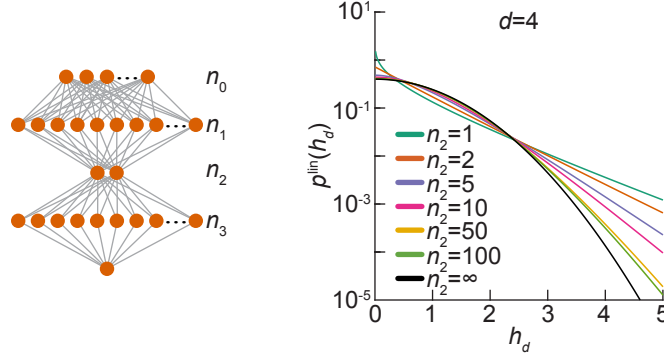


Figure 2: Priors of depth $d = 4$ linear networks with narrow bottlenecks. The left panel shows a diagram of a depth $d = 4$ network with two wide hidden layers of widths n_1 and n_3 separated by a narrow bottleneck of width $n_2 = 2$. The right panel shows prior densities for networks of this structure with $n_1 = n_3 = 100$ and variable bottleneck widths n_2 , which is indicated by line color. The prior density is plotted only for positive values of the output preactivation h_d , as it is symmetric about zero. The black line indicates the Gaussian limit in which the widths of all three hidden layers are taken to infinity, as discussed in §4.3. Further details on the numerical methods used to generate this figure are provided in Appendix E.

we can use G -function identities to recover our earlier results (10) and (11) for a two-layer network (see Appendix A) [29]. We plot the exact density for networks of depths $d = 2, 3$, and 4 and various widths along with densities estimated from numerical sampling in Figure 1, illustrating that our exact result displays the expected perfect agreement with experiment (see Appendix E for details of our numerical methods).

For any depth, the density (14) has the intriguing property that its functional form depends only on the difference between the hidden layer widths and the output dimensionality. This suggests that the priors of networks with large input and output dimensionalities but narrow intermediate bottlenecks—as would be the case for an autoencoder—will differ noticeably from those of networks with only a few outputs. However, it is challenging to visualize a distribution over more than two variables. We therefore plot the marginal prior over a single component of the output of a network with a bottleneck layer of varying width in Figure 2. Qualitatively, the prior for a network with a narrow bottleneck layer sandwiched between two wide hidden layers is more similar to that of a uniformly narrow network than that of a wide network without a bottleneck. These observations are consistent with previous arguments that wide networks with narrow bottlenecks may possess interesting priors [9, 35].

3.3 Deep ReLU networks

Finally, we consider ReLU networks. For this purpose, we adopt a more verbose notation in which the dependence of the prior on width is explicitly indicated, writing $p_d^{\text{lin}}(\mathbf{h}_d; \kappa_d; n_1, \dots, n_{d-1}, n_d)$ for the prior density (14) of a linear network with the specified hidden layer widths. Similarly, we write $p_d^{\text{ReLU}}(\mathbf{h}_d; \kappa_d; n_1, \dots, n_{d-1}, n_d)$ for the prior density of the corresponding ReLU network. As shown in Appendix B, we find that

$$\begin{aligned}
p_d^{\text{ReLU}}(\mathbf{h}_d; \kappa_d; n_1, \dots, n_d) &= \left(1 - \frac{(2^{n_1} - 1)(2^{n_2} - 1) \cdots (2^{n_{d-1}} - 1)}{2^{n_1 + \cdots + n_{d-1}}}\right) \delta(\mathbf{h}_d) \\
&\quad + \frac{1}{2^{n_1 + \cdots + n_{d-1}}} \sum_{k_1=1}^{n_1} \cdots \sum_{k_{d-1}=1}^{n_{d-1}} \binom{n_1}{k_1} \cdots \binom{n_{d-1}}{k_{d-1}} p_d^{\text{lin}}(\mathbf{h}_d; \kappa_d; k_1, \dots, k_{d-1}, n_d), \quad (16)
\end{aligned}$$

where $\delta(\mathbf{h}_d)$ is the n_d -dimensional Dirac distribution. We prove this result by induction on network depth d , using the characteristic function corresponding to this density. The base case $d = 2$ follows by direct integration and the binomial theorem, and the inductive step uses the fact that the linear

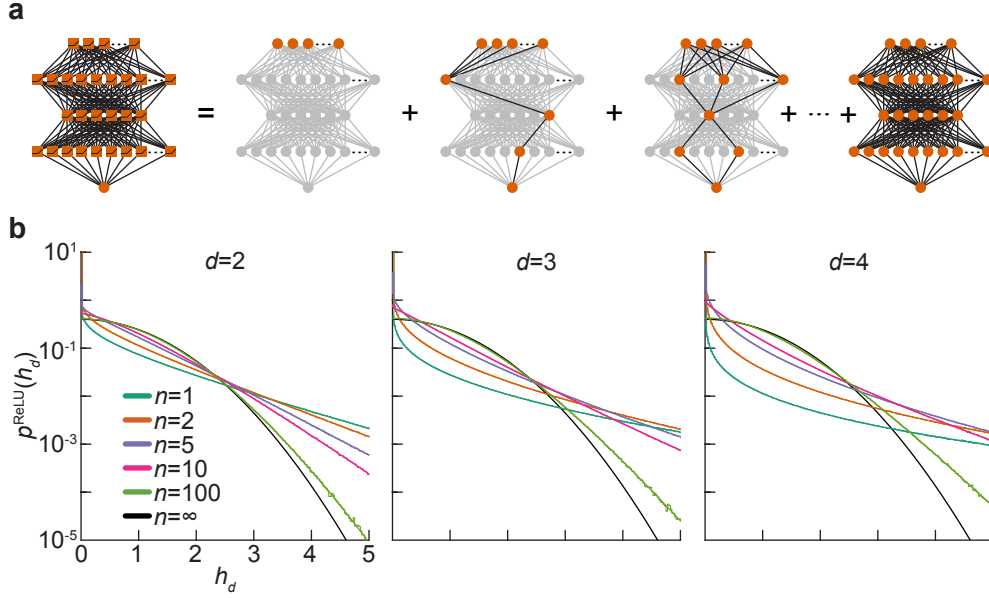


Figure 3: The prior of a deep ReLU network. **(a)** Schematic depiction of the ReLU prior as a mixture of the priors of linear networks of different widths (16). Grey nodes indicate ‘inactive’ units, while the linear network of active units is shown by the orange nodes. **(b)** ReLU prior densities for networks of depths $d = 2, 3$, and 4 and varying width. Here, we choose κ_d such that the variance of the preactivations matches that of the linear networks shown in Figure 1. In each panel, the prior density is plotted only for positive values of the output preactivation h_d , as it is symmetric about zero. For each depth, all hidden layers are of the same width n , which is indicated by line color. The black line indicates the Gaussian infinite-width limit discussed in §4.3. Thick lines show the exact priors, while thin jagged lines show experimental estimates from 10^8 examples. Further details on the numerical methods used to generate these figures are provided in Appendix E.

network prior (14) is radial and has marginals equal to the priors of linear networks with fewer outputs. This result has a simple interpretation: the prior for a ReLU network is a mixture of priors of linear networks corresponding to different numbers of active ReLU units in each hidden layer, along with a Dirac distribution representing the cases in which no output units are active. As we did for linear networks, we plot the exact density along with numerical estimates in Figure 3, showing perfect agreement.

4 Properties of these priors

Having obtained exact expressions for the priors of deep linear or ReLU networks, we briefly characterize their properties, and how those properties relate to prior analyses of finite network priors.

4.1 Moments

We first consider the moments of the output preactivation. As the prior distributions are zero-centered and isotropic, it is clear that all odd raw moments vanish. However, the moments of the norm of the output preactivation are non-vanishing. In particular, using basic properties of the Meijer G -function [28, 29], we can easily read off the moments for a linear network as

$$\mathbb{E}_{\text{lin}} \|\mathbf{h}_d\|^m = 2^{dm/2} \kappa_d^m \prod_{\ell=1}^d \left(\frac{n_\ell}{2} \right)^{\overline{m/2}} \quad (m \geq 0), \quad (17)$$

where $a^{\bar{b}} = \Gamma(a+b)/\Gamma(a)$ is the rising factorial [28]. This result takes a particularly simple form for the even moments $m = 2k$, in which case $(n/2)^{\bar{k}} = 2^{-k} \prod_{j=0}^{k-1} (n+2j)$. Most simply, for $m = 2$, we have $\mathbb{E}_{\text{lin}} \|\mathbf{h}_d\|^2 = \kappa_d^2 n_1 \cdots n_d$.

Similarly, for ReLU networks, we have

$$\mathbb{E}_{\text{ReLU}} \|\mathbf{h}_d\|^m = 2^{dm/2} \kappa_d^m \left(\frac{n_d}{2}\right)^{\overline{m/2}} \prod_{\ell=1}^{d-1} \left[\frac{1}{2^{n_\ell}} \sum_{k_\ell=1}^{n_\ell} \binom{n_\ell}{k_\ell} \left(\frac{k_\ell}{2}\right)^{\overline{m/2}} \right]. \quad (18)$$

Each term in the product over ℓ expands in terms of generalized hypergeometric functions evaluated at unity [28]. As for linear networks, this expression has a particularly simple form for even moments, particularly if $m = 2$, for which $\mathbb{E}_{\text{ReLU}} \|\mathbf{h}_d\|^2 = 2^{1-d} \kappa_d^2 n_1 \cdots n_d$. Therefore, for identical weight variances, the variance of the output preactivation of a ReLU network is 2^{1-d} times that of a linear network of the same width and depth. However, one can compensate for this variance reduction by simply doubling the variances of the priors over the hidden layer weights.

Using the property that the marginal prior distribution of a single component of the output is identical to the prior of a single-output network, these results give the marginal absolute moments of the prior of a linear or ReLU network. Moreover, these results can also be used to obtain joint moments of different components by exploiting the fact that the prior is radial. By symmetry, the odd moments vanish, and the even moments are given up to combinatorial factors by the corresponding moments of any individual component of the preactivation. For example, the covariance of two components of the output preactivation is $\mathbb{E} h_{d,i} h_{d,j} = (\mathbb{E} h_{d,1}^2) \delta_{ij}$ for all $i, j = 1, \dots, n_d$.

4.2 Tail bounds

Vladimirova et al. [21, 22] have shown that the marginal prior distributions of the preactivations of deep networks with ReLU-like activation functions and fixed, finite widths become increasingly heavy-tailed with depth. This behavior contrasts sharply with the thin-tailed Gaussian prior of infinite-width networks [4–8]. In particular, Vladimirova et al. [21, 22] showed that the prior distributions are sub-Weibull with optimal tail parameter $\theta = d/2$, meaning that they satisfy

$$\mathbb{P}(|h_{d,j}| \geq \rho) \leq C \exp(-\rho^{1/\theta}) \quad (19)$$

for each neuron $j \in \{1, \dots, n_d\}$, all $\rho > 0$, and some constant $C > 0$ if $\theta \geq d/2$, but not if $\theta < d/2$. A sub-Gaussian distribution is sub-Weibull with optimal tail parameter at most $1/2$; distributions with larger tail parameters have increasingly heavy tails. As shown in Appendix C, we can use the results of §4.1 to give a straightforward derivation of this result, showing that the norm $\|\mathbf{h}_d\|$ of the output preactivation for either linear or ReLU networks is sub-Weibull with optimal tail parameter $d/2$. Due to the aforementioned fact that the marginal prior for a single output of a multi-output network is identical to the prior for a single-output network, this implies (19).

4.3 Asymptotic behavior

Most previous studies of the priors of deep Bayesian networks have focused on their asymptotic behavior for large hidden layer widths. Provided that one takes

$$\kappa_d = (n_1 \cdots n_{d-1})^{-1/2} \varkappa_d \quad (20)$$

for \varkappa_d independent of the hidden layer widths such that the preactivation variance remains finite, the prior tends to a Gaussian as $n_1, \dots, n_{d-1} \rightarrow \infty$ for fixed d , n_0 , and n_d [4–10, 12, 24]. This behavior is qualitatively apparent in Figures 1 and 3. Here, we exploit our exact results to study this asymptotic regime. An ideal approach would be to study the asymptotic behavior of the characteristic function (13) and apply Lévy’s continuity theorem [36] to obtain the Gaussian limit, but we are not aware of suitable doubly-scaled asymptotic expansions for the Meijer G -function [28, 29]. Instead, we use a multivariate Edgeworth series to obtain an asymptotic expansion of the density [37]. As

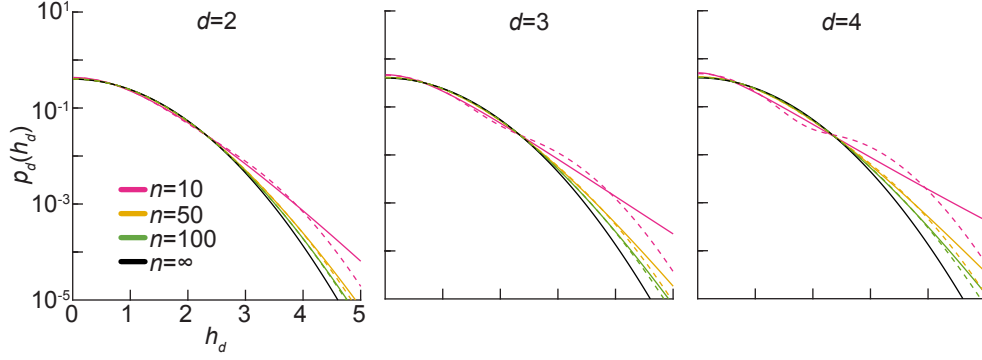


Figure 4: The large-width Edgeworth approximation for the prior density is thin-tailed. From left to right, the panels show the priors of linear networks of depths $d = 2, 3$, and 4 of varying widths. In each panel, solid lines show the exact prior density (14), while dashed lines show the asymptotic Edgeworth approximation (21). The exact prior density is computed numerically as described in Appendix E.

detailed in Appendix D, we find that the prior of a linear network has an Edgeworth series of the form

$$p_d^{\text{lin}}(\mathbf{h}_d | \mathbf{x}) \approx \frac{1}{(2\pi\mathcal{V}_d^2)^{n_d/2}} \exp\left(-\frac{\|\mathbf{h}_d\|^2}{2\mathcal{V}_d^2}\right) \times \left[1 + \frac{1}{4} \left(\sum_{\ell=1}^{d-1} \frac{1}{n_\ell}\right) \left(\frac{\|\mathbf{h}_d\|^4}{\mathcal{V}_d^4} - 2(n_d + 2)\frac{\|\mathbf{h}_d\|^2}{\mathcal{V}_d^2} + n_d(n_d + 2)\right) + \mathcal{O}\left(\frac{1}{n^2}\right)\right]. \quad (21)$$

The Edgeworth expansion of the prior of a ReLU network is of the same form, with the factor of $1/4$ scaling the finite-width correction being replaced by $5/4$, and the variance \mathcal{V}_d^2 re-scaled by 2^{1-d} . Heuristically, this result makes sense given that the binomial sums in (16) will be dominated by $k_\ell \approx n_\ell/2$ in the large-width limit.

These results succinctly reproduce the leading finite-width corrections formally written down by Antognini [15] and recursively computed by Yaida [12]. However, importantly, this approximate distribution is sub-Gaussian: it cannot capture the depth-dependent heaviness of the tails of the true finite-width prior described in §4.2. More generally, one can see that the heavier-than-Gaussian tails of the finite width prior are an essentially non-perturbative effect. At any finite order of the Edgeworth expansion, the approximate density for a network of any fixed depth is of the form $(2\pi\mathcal{V}_d^2)^{-n_d/2} \exp(-\|\mathbf{h}_d\|^2/2\mathcal{V}_d^2)[1 + f(\|\mathbf{h}_d\|^2/\mathcal{V}_d^2)]$, where f is a polynomial satisfying $\int d\mathbf{h} \exp(-\|\mathbf{h}\|^2/2) f(\|\mathbf{h}\|^2) = 0$ [37]. Such a density is sub-Gaussian. In Figure 4, we illustrate the discrepancy between the thin tails of the Edgeworth expansion and the heavier tails of the exact prior. Even at the relatively modest depths shown, the increasing discrepancy between the tail behavior of the approximate prior and the true tail behavior with increasing depth is clearly visible. We emphasize that low-order Edgeworth expansions will capture some qualitative features of the finite-width prior, but not all. It is therefore important to consider approximation accuracy on a case-by-case basis depending on what features of finite BNNs one aims to study.

5 Related work

As previously mentioned, our work closely relates to a program that proposes to study finite BNNs perturbatively by calculating asymptotic corrections to the prior [12, 14]. Though these approaches are applicable to the prior over outputs for multiple input examples and to more general activation functions, they are valid only in the regime of large hidden layer widths. As detailed in §4.3, these asymptotic results can be obtained as a limiting case of our exact solutions, though the Edgeworth series does not capture the heavier-than-Gaussian tails of the true finite-width prior. In a similar vein, recent works have perturbatively studied the finite-width posterior for a Gaussian likelihood

[12, 13, 38]. Our work is particularly similar in spirit to that of Schoenholz et al. [13], who considered asymptotic approximations to the partition function of the single-example function space posterior. Our exact solutions for simple models provide a broadly useful point of comparison for future perturbative study [12–15, 25–27].

As discussed in §4.2, our exact results recapitulate the observation of Vladimirova et al. [21, 22] that the prior distributions of finite networks become increasingly heavy-tailed with depth. Moreover, our results are consistent with the work of Gur-Ari and colleagues, who showed that the moments we compute should remain bounded at large widths [16, 17]. Similar results on the tail behavior of deep Gaussian processes, of which BNNs are a degenerate subclass, have recently been obtained by Lu et al. [39] and by Pleiss and Cunningham [40]. Our approach complements the study of tail bounds and asymptotic moments. Exact solutions provide a finer-grained characterization of the prior, but it is possible to compute tail bounds and moments for models for which the exact prior is not straightforwardly calculable. We note that, following the appearance of our work in preprint form and after the submission deadline, parallel results on exact marginal function-space priors were announced by Noci et al. [41].

After the completion of our work, we became aware of the close connection of our results on deep linear network priors to previous work in random matrix theory (RMT). In the language of RMT, the marginal function-space prior of a deep linear BNN is a particular linear statistic of the product of rectangular real Ginibre matrices (i.e., matrices with independent and identically distributed Gaussian entries) [42]. An alternative proof of the result (14) then follows by using the rotational invariance of what is known in RMT as the one-point weight function of the singular value distribution of the product matrix [43]. However, to the best of our knowledge, this connection had not previously been exploited to study the properties of finite linear BNNs. Further non-asymptotic study of random matrix products, and of nonlinear compositions as in the deep ReLU BNNs considered here, will be an interesting objective for future work [42–44].

Finally, previous works have theoretically and empirically investigated how finite-width network priors affect inference [9–11, 18–20, 23]. Some of these studies observed an intriguing phenomenon: better generalization performance is obtained when inference is performed using a “cold” posterior that is artificially tempered as $p(\mathbf{h}_d | \mathbf{x}, \mathbf{y})^{1/T}$ for $0 < T < 1$ [11, 18, 19]. This contravenes the expectation that the Bayes posterior (i.e., $T = 1$) should be optimal. It has been suggested that this effect reflects misspecification either of the prior over the weights—namely, that a distribution other than an isotropic Gaussian should be employed—or of the likelihood [11], but the true cause remains unclear [20]. The exact function space priors computed in this work should prove useful in ongoing dissections of simple models for BNN inference. Most simply, they provide a finer-grained understanding of how hyperparameter choice affects the prior than that afforded by tail bounds alone [21, 22, 40]. Though we do not compute function-space posterior distributions, knowing the precise form of the prior would allow one to gain an intuitive understanding of the shape of the posterior for a given likelihood [10]. For instance, one could imagine a particular degree of heavy-tailedness in the prior being optimal for a dataset that is to some degree heavy-tailed. This could allow one to gain some intuition for when the prior or likelihood is misspecified for a given dataset. Detailed experimental and analytical investigation of these questions is an important objective of our future work.

6 Conclusions

In this paper, we have performed the first exact characterization of the function-space priors of finite deep Bayesian neural networks induced by Gaussian priors over their weights. These exact solutions provide a useful check on the validity of perturbative studies [12, 14, 15], and unify previous descriptions of finite-width network priors [12, 14–17, 21, 22]. Our solutions were, however, obtained for the relatively restrictive setting of the marginal prior for a single input example of a feedforward network with no bias terms. As our approach relies heavily on rotational invariance, it is unclear how best to generalize these methods to networks with non-zero bias terms, or to the joint prior of the output preactivations for multiple inputs. We therefore leave detailed study of those general settings as an interesting objective for future work.

Acknowledgments and Disclosure of Funding

We thank A. Atanasov, B. Bordelon, A. Canatar, and M. Farrell for helpful comments on our manuscript. The computations in this paper were performed using the Harvard University FAS Division of Science Research Computing Group’s Cannon HPC cluster. JAZ-V acknowledges support from the NSF-Simons Center for Mathematical and Statistical Analysis of Biology at Harvard and the Harvard Quantitative Biology Initiative. CP thanks Intel, Google, and the Harvard Data Science Initiative for support. The authors declare no competing interests.

References

- [1] David JC MacKay. A practical Bayesian framework for backpropagation networks. *Neural Computation*, 4(3):448–472, 1992.
- [2] Ian Goodfellow, Yoshua Bengio, Aaron Courville, and Yoshua Bengio. *Deep learning*. MIT Press, Cambridge, MA, USA, 2016.
- [3] Yann LeCun, Yoshua Bengio, and Geoffrey Hinton. Deep learning. *Nature*, 521(7553):436–444, 2015.
- [4] Radford M Neal. Priors for infinite networks. In *Bayesian Learning for Neural Networks*, pages 29–53. Springer, 1996.
- [5] Christopher KI Williams. Computing with infinite networks. *Advances in Neural Information Processing Systems*, pages 295–301, 1997.
- [6] Alexander G. de G. Matthews, Jiri Hron, Mark Rowland, Richard E. Turner, and Zoubin Ghahramani. Gaussian process behaviour in wide deep neural networks. In *International Conference on Learning Representations*, 2018. URL <https://openreview.net/forum?id=H1-nGgWC->.
- [7] Jaehoon Lee, Jascha Sohl-Dickstein, Jeffrey Pennington, Roman Novak, Sam Schoenholz, and Yasaman Bahri. Deep neural networks as Gaussian processes. In *International Conference on Learning Representations*, 2018. URL <https://openreview.net/forum?id=B1EA-M-0Z>.
- [8] Greg Yang. Scaling limits of wide neural networks with weight sharing: Gaussian process behavior, gradient independence, and neural tangent kernel derivation. *arXiv preprint arXiv:1902.04760*, 2019.
- [9] Laurence Aitchison. Why bigger is not always better: on finite and infinite neural networks. In Hal Daumé III and Aarti Singh, editors, *Proceedings of the 37th International Conference on Machine Learning*, volume 119 of *Proceedings of Machine Learning Research*, pages 156–164. PMLR, July 2020. URL <http://proceedings.mlr.press/v119/aitchison20a.html>.
- [10] Andrew Gordon Wilson and Pavel Izmailov. Bayesian deep learning and a probabilistic perspective of generalization. *arXiv preprint arXiv:2002.08791*, 2020.
- [11] Laurence Aitchison. A statistical theory of cold posteriors in deep neural networks. In *International Conference on Learning Representations*, 2021. URL <https://openreview.net/forum?id=Rd138pWXMvG>.
- [12] Sho Yaida. Non-Gaussian processes and neural networks at finite widths. In Jianfeng Lu and Rachel Ward, editors, *Proceedings of The First Mathematical and Scientific Machine Learning Conference*, volume 107 of *Proceedings of Machine Learning Research*, pages 165–192, Princeton University, Princeton, NJ, USA, July 2020. PMLR. URL <http://proceedings.mlr.press/v107/yaida20a.html>.
- [13] Samuel S Schoenholz, Jeffrey Pennington, and Jascha Sohl-Dickstein. A correspondence between random neural networks and statistical field theory. *arXiv preprint arXiv:1710.06570*, 2017.
- [14] James Halverson, Anindita Maiti, and Keegan Stoner. Neural networks and quantum field theory. *Machine Learning: Science and Technology*, 2021.

- [15] Joseph M Antognini. Finite size corrections for neural network Gaussian processes. *arXiv preprint arXiv:1908.10030*, 2019.
- [16] Ethan Dyer and Guy Gur-Ari. Asymptotics of wide networks from Feynman diagrams. In *International Conference on Learning Representations*, 2020. URL <https://openreview.net/forum?id=SigFvANKDS>.
- [17] Kyle Aitken and Guy Gur-Ari. On the asymptotics of wide networks with polynomial activations. *arXiv preprint arXiv:2006.06687*, 2020.
- [18] Florian Wenzel, Kevin Roth, Bastiaan Veeling, Jakub Swiatkowski, Linh Tran, Stephan Mandt, Jasper Snoek, Tim Salimans, Rodolphe Jenatton, and Sebastian Nowozin. How good is the Bayes posterior in deep neural networks really? In Hal Daumé III and Aarti Singh, editors, *Proceedings of the 37th International Conference on Machine Learning*, volume 119 of *Proceedings of Machine Learning Research*, pages 10248–10259. PMLR, 13–18 Jul 2020. URL <http://proceedings.mlr.press/v119/wenzel20a.html>.
- [19] Vincent Fortuin, Adrià Garriga-Alonso, Florian Wenzel, Gunnar Rätsch, Richard Turner, Mark van der Wilk, and Laurence Aitchison. Bayesian neural network priors revisited. *arXiv preprint arXiv:2102.06571*, 2021.
- [20] Pavel Izmailov, Sharad Vikram, Matthew D Hoffman, and Andrew Gordon Gordon Wilson. What are bayesian neural network posteriors really like? In Marina Meila and Tong Zhang, editors, *Proceedings of the 38th International Conference on Machine Learning*, volume 139 of *Proceedings of Machine Learning Research*, pages 4629–4640. PMLR, 18–24 Jul 2021. URL <http://proceedings.mlr.press/v139/izmailov21a.html>.
- [21] Mariia Vladimirova, Jakob Verbeek, Pablo Mesejo, and Julyan Arbel. Understanding priors in Bayesian neural networks at the unit level. In Kamalika Chaudhuri and Ruslan Salakhutdinov, editors, *Proceedings of the 36th International Conference on Machine Learning*, volume 97 of *Proceedings of Machine Learning Research*, pages 6458–6467. PMLR, 09–15 Jun 2019. URL <http://proceedings.mlr.press/v97/vladimirova19a.html>.
- [22] Mariia Vladimirova, Stéphane Girard, Hien Nguyen, and Julyan Arbel. Sub-Weibull distributions: Generalizing sub-Gaussian and sub-Exponential properties to heavier tailed distributions. *Stat*, 9(1):e318, 2020. doi: <https://doi.org/10.1002/sta4.318>. URL <https://onlinelibrary.wiley.com/doi/abs/10.1002/sta4.318>. e318 sta4.318.
- [23] Jaehoon Lee, Samuel S Schoenholz, Jeffrey Pennington, Ben Adlam, Lechao Xiao, Roman Novak, and Jascha Sohl-Dickstein. Finite versus infinite neural networks: an empirical study. *arXiv preprint arXiv:2007.15801*, 2020.
- [24] Greg Yang and Edward J Hu. Feature learning in infinite-width neural networks. *arXiv preprint arXiv:2011.14522*, 2020.
- [25] Rodney J Baxter. *Exactly solved models in statistical mechanics*. Dover Publications, Mineola, New York, 2007.
- [26] Barry M McCoy and Tai Tsun Wu. *The two-dimensional Ising model*. Courier Corporation, 2014.
- [27] Carl M Bender and Tai Tsun Wu. Anharmonic oscillator. *Physical Review*, 184(5):1231, 1969.
- [28] DLMF. *NIST Digital Library of Mathematical Functions*. <http://dlmf.nist.gov/>, Release 1.1.1 of 2021-03-15, 2021. URL <http://dlmf.nist.gov/>. F. W. J. Olver, A. B. Olde Daalhuis, D. W. Lozier, B. I. Schneider, R. F. Boisvert, C. W. Clark, B. R. Miller, B. V. Saunders, H. S. Cohl, and M. A. McClain, eds.
- [29] Arthur Erdélyi, Wilhelm Magnus, Fritz Oberhettinger, and Francesco G. Tricomi. *Higher Transcendental Functions. Vol. I*. McGraw-Hill Book Company, Inc., New York-Toronto-London, 1953. URL <https://authors.library.caltech.edu/43491/>. Reprinted by Robert E. Krieger Publishing Co. Inc., 1981. Table errata: Math. Comp. v. 65 (1996), no. 215, p. 1385, v. 41 (1983), no. 164, p. 778, v. 30 (1976), no. 135, p. 675, v. 25 (1971), no. 115, p. 635, v. 25 (1971), no. 113, p. 199, v. 24 (1970), no. 112, p. 999, v. 24 (1970), no. 110, p. 504, v. 17 (1963), no. 84, p. 485.

- [30] Arthur Erdélyi, Wilhelm Magnus, Fritz Oberhettinger, and Francesco G. Tricomi. *Tables of Integral Transforms. Vol. I.* McGraw-Hill Book Company, Inc., New York-Toronto-London, 1954. URL <https://authors.library.caltech.edu/43489/>. Table errata: Math. Comp. v. 66 (1997), no. 220, p. 1766–1767, v. 65 (1996), no. 215, p. 1384, v. 50 (1988), no. 182, p. 653, v. 41 (1983), no. 164, p. 778–779, v. 27 (1973), no. 122, p. 451, v. 26 (1972), no. 118, p. 599, v. 25 (1971), no. 113, p. 199, v. 24 (1970), no. 109, p. 239–240.
- [31] Arthur Erdélyi, Wilhelm Magnus, Fritz Oberhettinger, and Francesco G. Tricomi. *Tables of Integral Transforms. Vol. II.* McGraw-Hill Book Company, Inc., New York-Toronto-London, 1954. URL <https://authors.library.caltech.edu/43489/>. Table errata: Math. Comp. v. 65 (1996), no. 215, p. 1385, v. 41 (1983), no. 164, pp. 779–780, v. 31 (1977), no. 138, p. 614, v. 31 (1977), no. 137, pp. 328–329, v. 26 (1972), no. 118, p. 599, v. 25 (1971), no. 113, p. 199, v. 23 (1969), no. 106, p. 468.
- [32] Izrail Solomonovich Gradshteyn and Iosif Moiseevich Ryzhik. *Table of integrals, series, and products.* Academic Press, 2014.
- [33] Elias M Stein and Guido Weiss. *Introduction to Fourier Analysis on Euclidean Spaces (PMS-32), Volume 32.* Princeton University Press, 2016.
- [34] Samuel Kotz, Tomasz Kozubowski, and Krzysztof Podgorski. *The Laplace distribution and generalizations: a revisit with applications to communications, economics, engineering, and finance.* Springer Science & Business Media, 2012.
- [35] Devanshu Agrawal, Theodore Papamarkou, and Jacob Hinkle. Wide neural networks with bottlenecks are deep gaussian processes. *Journal of Machine Learning Research*, 21(175):1–66, 2020. URL <http://jmlr.org/papers/v21/20-017.html>.
- [36] David Pollard. *A user’s guide to measure theoretic probability*, volume 8. Cambridge University Press, 2002.
- [37] Ib M Skovgaard. On multivariate Edgeworth expansions. *International Statistical Review/Revue Internationale de Statistique*, pages 169–186, 1986.
- [38] Gadi Naveh, Oded Ben-David, Haim Sompolsky, and Zohar Ringel. Predicting the outputs of finite networks trained with noisy gradients. *arXiv preprint arXiv:2004.01190*, 2020.
- [39] Chi-Ken Lu, Scott Cheng-Hsin Yang, Xiaoran Hao, and Patrick Shafto. Interpretable deep gaussian processes with moments. In Silvia Chiappa and Roberto Calandra, editors, *Proceedings of the Twenty Third International Conference on Artificial Intelligence and Statistics*, volume 108 of *Proceedings of Machine Learning Research*, pages 613–623. PMLR, 26–28 Aug 2020. URL <https://proceedings.mlr.press/v108/lu20b.html>.
- [40] Geoff Pleiss and John P Cunningham. The limitations of large width in neural networks: A deep Gaussian process perspective. *arXiv preprint arXiv:2106.06529*, 2021.
- [41] Lorenzo Noci, Gregor Bachmann, Kevin Roth, Sebastian Nowozin, and Thomas Hofmann. Precise characterization of the prior predictive distribution of deep ReLU networks. *arXiv preprint arXiv:2106.06615*, 2021.
- [42] Boris Hanin. Random neural networks in the infinite width limit as Gaussian processes. *arXiv preprint arXiv:2107.01562*, 2021.
- [43] Jesper R. Ipsen and Mario Kieburg. Weak commutation relations and eigenvalue statistics for products of rectangular random matrices. *Phys. Rev. E*, 89:032106, Mar 2014. doi: 10.1103/PhysRevE.89.032106. URL <https://link.aps.org/doi/10.1103/PhysRevE.89.032106>.
- [44] Boris Hanin and Grigoris Paouris. Non-asymptotic results for singular values of Gaussian matrix products. *Geometric and Functional Analysis*, 31(2):268–324, 2021.

Supplemental Information

A Derivation of the prior of a deep linear network

In this appendix, we prove the formula for the prior of a deep linear network given in §3.2. In §A.1, we prove that the claimed density and characteristic function are indeed a Fourier transform pair using identities for the Hankel transform, and then prove by induction that these results describe the prior of a deep linear network in §A.2. Finally, we provide a lengthier, albeit possibly more transparent, proof of these results by direct integration in §A.3.

A.1 Fourier transforms of radial functions and the Hankel transform

We begin by reviewing the relationship between the Fourier transform of a radial function and the Hankel transform, and then use this relationship to prove that the claimed characteristic function and density are a Fourier transform pair. Let $p, \varphi : \mathbb{R}^n \rightarrow \mathbb{R}$ be a Fourier transform pair, with

$$\varphi(\mathbf{q}) = \int d\mathbf{h} \exp(-i\mathbf{h} \cdot \mathbf{q}) p(\mathbf{h}) \quad \text{and} \quad p(\mathbf{h}) = \int \frac{d\mathbf{q}}{(2\pi)^n} \exp(i\mathbf{h} \cdot \mathbf{q}) \varphi(\mathbf{q}). \quad (\text{A.1})$$

Assume that p and φ are radial functions, i.e., that $p(\mathbf{h}) = p(\|\mathbf{h}\|)$ and $\varphi(\mathbf{q}) = \varphi(\|\mathbf{q}\|)$. We note that if one of p or φ is radial, it follows that both are radial [33]. Then, we have the Hankel transform relations

$$\varphi(\mathbf{q}) = (2\pi)^{+n/2} \|\mathbf{q}\|^{(2-n)/2} \int_0^\infty r dr J_{(n-2)/2}(\|\mathbf{q}\|r) r^{(n-2)/2} p(r) \quad (\text{A.2})$$

$$p(\mathbf{h}) = (2\pi)^{-n/2} \|\mathbf{h}\|^{(2-n)/2} \int_0^\infty r dr J_{(n-2)/2}(\|\mathbf{h}\|r) r^{(n-2)/2} \varphi(r), \quad (\text{A.3})$$

where $J_\nu(z)$ is the Bessel function of the first kind of order ν [28, 33, 29–31]. We note that inversion of the Hankel transform formally follows from the distributional identity

$$\int_0^\infty r dr J_\nu(kr) J_\nu(k'r) = \frac{\delta(k - k')}{k} \quad (\text{A.4})$$

for $k, k' > 0$ [28, 33, 29–31].

We now use this relationship to show that

$$p_d^{\text{lin}}(\mathbf{h}_d | \mathbf{x}) = \frac{\gamma_d}{(2^d \pi \kappa_d^2)^{n_d/2}} G_{0,d}^{d,0} \left(\frac{\|\mathbf{h}_d\|^2}{2^d \kappa_d^2} \middle| 0, (n_1 - n_d)/2, \dots, (n_{d-1} - n_d)/2 \right) \quad (\text{A.5})$$

and

$$\varphi_d^{\text{lin}}(\mathbf{q}_d | \mathbf{x}) = \gamma_d G_{d-1,1}^{1,d-1} \left(2^{d-2} \kappa_d^2 \|\mathbf{q}_d\|^2 \middle| 1 - n_1/2, \dots, 1 - n_{d-1}/2 \right) \quad (\text{A.6})$$

are a Fourier transform pair, where $\kappa_d, \gamma_d > 0$ and $n_1, \dots, n_d \in \mathbb{N}_{>0}$. As both of these G -functions are well-behaved, it suffices to show one direction of this relationship; we will show that p_d is the inverse Fourier transform of φ_d . Our starting point is the formula for the Hankel transform of a G -function multiplied by a power:

$$\int_0^\infty dx J_\nu(xy) x^{2\rho} G_{p,q}^{m,n} \left(\lambda x^2; \begin{matrix} a_1, \dots, a_p \\ b_1, \dots, b_q \end{matrix} \right) = \frac{2^{2\rho}}{y^{2\rho+1}} G_{p+2,q}^{m,n+1} \left(\frac{4\lambda}{y^2}; \begin{matrix} h, a_1, \dots, a_p, k \\ b_1, \dots, b_q \end{matrix} \right) \quad (\text{A.7})$$

where $h = 1/2 - \rho - \nu/2$ and $k = 1/2 - \rho + \nu/2$, valid for $p + q < 2(m + n)$, all real λ , $\Re(b_j + \rho + \nu/2) > -1/2$, and $\Re(a_j + \rho) < 3/4$ [31]. Using this identity and simplifying the result using the G -function identities [28, 29]

$$G_{p,q}^{m,n} \left(\frac{1}{z} \middle| \begin{matrix} a_1, \dots, a_p \\ b_1, \dots, b_q \end{matrix} \right) = G_{q,p}^{n,m} \left(z \middle| \begin{matrix} 1 - b_1, \dots, 1 - b_q \\ 1 - a_1, \dots, 1 - a_p \end{matrix} \right) \quad (\text{A.8})$$

and

$$z^\mu G_{p,q}^{m,n} \left(z \middle| \begin{matrix} a_1, \dots, a_p \\ b_1, \dots, b_q \end{matrix} \right) = G_{p,q}^{m,n} \left(z \middle| \begin{matrix} a_1 + \mu, \dots, a_p + \mu \\ b_1 + \mu, \dots, b_q + \mu \end{matrix} \right), \quad (\text{A.9})$$

we obtain

$$p_d^{\text{lin}}(\mathbf{h}_d | \mathbf{x}) = \frac{\gamma_d}{(2^d \kappa_d^2)^{n_d/2}} G_{1,d+1}^{d,1} \left(\frac{\|\mathbf{h}_d\|^2}{2^d \kappa_d^2} \middle| 0, (n_1 - n_d)/2, \dots, (n_{d-1} - n_d)/2, 1 - n_d/2 \right). \quad (\text{A.10})$$

Then, further simplifying using the identity [28, 29]

$$G_{p+1,q+1}^{m,n+1} \left(z \middle| \alpha, a_1, \dots, a_p \atop b_1, \dots, b_q, \alpha \right) = G_{p,q}^{m,n} \left(z \middle| a_1, \dots, a_p \atop b_1, \dots, b_q \right), \quad (\text{A.11})$$

we conclude the desired result. The proof that φ_d is the Fourier transform of p_d can be derived by an analogous procedure.

A.2 Inductive proof of the G -function formula

We now prove the claimed formula for the prior by induction on the depth d . Using the identities [29]

$$G_{0,2}^{2,0} \left(z \middle| 0, (n_1 - n_2)/2 \right) = 2z^{(n_1 - n_2)/4} K_{(n_1 - n_2)/2}(2\sqrt{z}) \quad (\text{A.12})$$

and

$$G_{1,1}^{1,1} \left(z \middle| 1 - n_1/2 \atop 0 \right) = \Gamma\left(\frac{n_1}{2}\right) (1+z)^{-n_1/2}, \quad (\text{A.13})$$

the claim for the density and characteristic function for the base case $d = 2$ follow from the direct calculation in §3.1 of the main text, specifically equations (10) and (11).

For $d > 2$, we observe that the general formula for the characteristic function (9) implies the recursive integral relation

$$\varphi_{d+1}^{\text{lin}}(\mathbf{q}_{d+1} | \mathbf{x}) = \int d\mathbf{h}_d \exp\left(-\frac{1}{2}\sigma_{d+1}^2 \|\mathbf{h}_d\|^2 \|\mathbf{q}_{d+1}\|^2\right) p_d(\mathbf{h}_d | \mathbf{x}). \quad (\text{A.14})$$

On the induction hypothesis, this yields

$$\begin{aligned} \varphi_{d+1}^{\text{lin}}(\mathbf{q}_{d+1} | \mathbf{x}) &= \frac{\gamma_d}{(2^d \pi \kappa_d^2)^{n_d/2}} \int d\mathbf{h}_d \exp\left(-\frac{1}{2}\sigma_{d+1}^2 \|\mathbf{h}_d\|^2 \|\mathbf{q}_{d+1}\|^2\right) \\ &\quad \times G_{0,d}^{d,0} \left(\frac{\|\mathbf{h}_d\|^2}{2^d \kappa_d^2} \middle| 0, \nu_1, \dots, \nu_{d-1} \right), \end{aligned} \quad (\text{A.15})$$

where we define $\nu_\ell \equiv (n_\ell - n_d)/2$ for $\ell = 1, \dots, d-1$ for brevity. Converting to spherical coordinates and evaluating the trivial angular integral, we have

$$\varphi_{d+1}^{\text{lin}}(\mathbf{q}_{d+1} | \mathbf{x}) = \gamma_{d+1} \int_0^\infty dt t^{n_d/2-1} \exp(-2^{d-1} \kappa_{d+1}^2 \|\mathbf{q}_{d+1}\|^2 t) G_{0,d}^{d,0} \left(t \middle| 0, \nu_1, \dots, \nu_{d-1} \right), \quad (\text{A.16})$$

where we have made the change of variables $t \equiv h_d^2/2^d \kappa_d^2$ and recognized $\kappa_{d+1} = \sigma_{d+1} \kappa_d$ and $\gamma_{d+1} = \gamma_d/\Gamma(n_d/2)$. We now recall the formula for the Laplace transform of a G -function multiplied by a power:

$$\int_0^\infty dt \exp(-zt) t^{-\alpha} G_{p,q}^{m,n} \left(t \middle| a_1, \dots, a_p \atop b_1, \dots, b_q \right) = z^{\alpha-1} G_{p+1,q}^{m,n+1} \left(\frac{1}{z} \middle| \alpha, a_1, \dots, a_p \atop b_1, \dots, b_q \right), \quad (\text{A.17})$$

valid either if $p + q < 2(m + n)$ and $\Re(\alpha) > \Re(b_j + 1)$ for all $j = 1, \dots, m$ or if $p < q$ and $\Re(\alpha) < \Re(b_j + 1)$ for all $j = 1, \dots, m$, and for $|\arg z| < (m + n - p/2 - q/2)\pi$ [30]. The latter condition applies, hence, using the identity (A.8), we find that

$$\begin{aligned} \varphi_{d+1}^{\text{lin}}(\mathbf{q}_{d+1} | \mathbf{x}) &= \gamma_{d+1} (2^{d-1} \kappa_{d+1}^2 \|\mathbf{q}_{d+1}\|^2)^{-n_d/2} \\ &\quad \times G_{d,1}^{1,d} \left(2^{d-1} \kappa_{d+1}^2 \|\mathbf{q}_{d+1}\|^2 \middle| 1, 1 - \nu_1, \dots, 1 - \nu_{d-1} \atop n_d/2 \right). \end{aligned} \quad (\text{A.18})$$

Then, applying the identity (A.9), we obtain

$$\varphi_{d+1}^{\text{lin}}(\mathbf{q}_{d+1} | \mathbf{x}) = \gamma_{d+1} G_{d,1}^{1,d} \left(2^{d-1} \kappa_{d+1}^2 \|\mathbf{q}_{d+1}\|^2 \middle| 1 - n_1/2, \dots, 1 - n_d/2 \atop 0 \right), \quad (\text{A.19})$$

where we have used the fact that the G -function is invariant under permutation of its upper arguments. Therefore, using the results of §A.1, we conclude the claimed result.

A.3 Derivation of the prior by direct integration

Here, we directly derive a formula for the prior as a $(d-1)$ -dimensional integral, and then show that this is equivalent to the expression in terms of the Meijer G -function. Separating out the terms that correspond to the first and last layers, the general expression for the characteristic function (9) becomes

$$\varphi_d^{\text{lin}}(\mathbf{q}_d) = \int \prod_{\ell=1}^{d-1} \frac{d\mathbf{q}_\ell d\mathbf{h}_\ell}{(2\pi)^{n_\ell}} \exp \left(\sum_{\ell=1}^{d-1} i\mathbf{q}_\ell \cdot \mathbf{h}_\ell - \frac{1}{2}\sigma_1^2 \|\mathbf{x}\|^2 \|\mathbf{q}_1\|^2 - \frac{1}{2} \sum_{\ell=2}^{d-1} \sigma_\ell^2 \|\mathbf{q}_\ell\|^2 \|\mathbf{h}_{\ell-1}\|^2 - \frac{1}{2} \sigma_d^2 \|\mathbf{q}_d\|^2 \|\mathbf{h}_{d-1}\|^2 \right), \quad (\text{A.20})$$

where we suppress the fact that φ_d is implicitly conditioned on \mathbf{x} . Transforming into spherical coordinates and evaluating the angular integrals as described in Appendix A.1, we obtain

$$\begin{aligned} \varphi_d^{\text{lin}}(\mathbf{q}_d) &= \left[\prod_{\ell=1}^{d-1} \frac{2^{1-n_\ell/2}}{\Gamma(n_\ell/2)} \right] \left[\prod_{\ell=1}^{d-1} \int_0^\infty dh_\ell \int_0^\infty dq_\ell (h_\ell q_\ell)^{n_\ell/2} J_{(n_\ell-2)/2}(h_\ell q_\ell) \right] \\ &\quad \times \exp \left(-\frac{1}{2}\sigma_1^2 \|\mathbf{x}\|^2 q_1^2 - \frac{1}{2} \sum_{\ell=2}^{d-1} \sigma_\ell^2 q_\ell^2 h_{\ell-1}^2 - \frac{1}{2} \sigma_d^2 \|\mathbf{q}_d\|^2 h_{d-1}^2 \right). \end{aligned} \quad (\text{A.21})$$

Assuming that $\sigma_\ell > 0$ and $\mathbf{x} \neq 0$, we make the change of variables

$$u_\ell \equiv \sigma_\ell \sigma_{\ell-1} \cdots \sigma_1 \|\mathbf{x}\| q_\ell \quad (\text{A.22})$$

$$v_\ell \equiv \frac{1}{\sigma_\ell \sigma_{\ell-1} \cdots \sigma_1 \|\mathbf{x}\|} h_\ell \quad (\text{A.23})$$

such that

$$\sigma_\ell^2 = u_\ell^2 v_{\ell-1}^2 \quad (\text{A.24})$$

and

$$q_\ell h_\ell = u_\ell v_\ell. \quad (\text{A.25})$$

This yields

$$\begin{aligned} \varphi_d^{\text{lin}}(\mathbf{q}_d) &= \left[\prod_{\ell=1}^{d-1} \frac{2^{1-n_\ell/2}}{\Gamma(n_\ell/2)} \right] \left[\prod_{\ell=1}^{d-1} \int_0^\infty dv_\ell \int_0^\infty du_\ell (v_\ell u_\ell)^{n_\ell/2} J_{(n_\ell-2)/2}(v_\ell u_\ell) \right] \\ &\quad \times \exp \left(-\frac{1}{2} u_1^2 - \frac{1}{2} \sum_{\ell=2}^{d-1} u_\ell^2 v_{\ell-1}^2 - \frac{1}{2} \kappa_d^2 v_{d-1}^2 \|\mathbf{q}_d\|^2 \right), \end{aligned} \quad (\text{A.26})$$

where we write

$$\kappa_d \equiv \sigma_d \sigma_{d-1} \cdots \sigma_1 \|\mathbf{x}\| \quad (\text{A.27})$$

for brevity.

At this stage, we shift to considering the prior density, following the results of §A.1. Using the identity [28, 32]

$$\int_0^\infty du_\ell u_\ell^{n_\ell/2} J_{(n_\ell-2)/2}(v_\ell u_\ell) \exp \left(-\frac{1}{2} v_{\ell-1}^2 u_\ell^2 \right) = v_\ell^{n_\ell/2-1} v_{\ell-1}^{-n_\ell} \exp \left(-\frac{1}{2} \frac{v_\ell^2}{v_{\ell-1}^2} \right) \quad (\text{A.28})$$

to integrate out the variables u_ℓ and q_d , we obtain

$$\begin{aligned} p_d^{\text{lin}}(\mathbf{h}_d) &= \frac{\kappa_d^{-n_d}}{(2\pi)^{n_d/2}} \left[\prod_{\ell=1}^{d-1} \frac{2^{1-n_\ell/2}}{\Gamma(n_\ell/2)} \right] \left[\prod_{\ell=1}^{d-1} \int_0^\infty dv_\ell v_\ell^{n_\ell-n_{\ell+1}-1} \right] \\ &\quad \times \exp \left(-\frac{1}{2} v_1^2 - \frac{1}{2} \sum_{\ell=2}^{d-1} \frac{v_\ell^2}{v_{\ell-1}^2} - \frac{1}{2} \frac{\|\mathbf{h}_d\|^2}{\kappa_d^2 v_{d-1}^2} \right). \end{aligned} \quad (\text{A.29})$$

We now make a change of variables to decouple all but one of the terms in the exponential. In particular, we let

$$s_\ell \equiv \begin{cases} v_1 & \ell = 1 \\ v_\ell/v_{\ell-1} & 1 < \ell \leq d-1, \end{cases} \quad (\text{A.30})$$

such that

$$v_\ell = s_\ell s_{\ell-1} \cdots s_1. \quad (\text{A.31})$$

The Jacobian of this transformation is lower triangular, and can be seen to have determinant

$$\left| \det \frac{\partial(v_1, \dots, v_{d-1})}{\partial(s_1, \dots, s_{d-1})} \right| = \frac{1}{s_1 s_2 \cdots s_{d-1}} \prod_{\ell=1}^{d-1} v_\ell, \quad (\text{A.32})$$

which is non-singular on all but a measure-zero subset of the integration domain. This yields

$$\left| \det \frac{\partial(v_1, \dots, v_{d-1})}{\partial(s_1, \dots, s_{d-1})} \right| \prod_{\ell=1}^{d-1} v_\ell^{n_\ell - n_{\ell+1} - 1} = \frac{1}{s_1 s_2 \cdots s_{d-1}} \prod_{\ell=1}^{d-1} v_\ell^{n_\ell - n_{\ell+1}} = \prod_{\ell=1}^{d-1} s_\ell^{n_\ell - n_d - 1}, \quad (\text{A.33})$$

hence the prior density becomes

$$p_d^{\text{lin}}(\mathbf{h}_d) = \frac{\kappa_d^{-n_d}}{(2\pi)^{n_d/2}} \left[\prod_{\ell=1}^{d-1} \frac{2^{1-n_\ell/2}}{\Gamma(n_\ell/2)} \right] \left[\prod_{\ell=1}^{d-1} \int_0^\infty ds_\ell s_\ell^{n_\ell - n_d - 1} \exp(-s_\ell^2/2) \right] \times \exp\left(-\frac{1}{2} \frac{\|\mathbf{h}_d\|^2}{\kappa_d^2} \frac{1}{s_1^2 s_2^2 \cdots s_{d-1}^2}\right). \quad (\text{A.34})$$

For convenience, we make a final change of variables

$$t_\ell \equiv \frac{1}{2} s_\ell^2, \quad (\text{A.35})$$

which yields the formula

$$p_d^{\text{lin}}(\mathbf{h}_d | \mathbf{x}) = \frac{\gamma_d}{(2^d \pi \kappa_d^2)^{n_d/2}} f_{d-1}\left(\frac{\|\mathbf{h}_d\|^2}{2^d \kappa_d^2}; \frac{n_1 - n_d}{2}, \dots, \frac{n_{d-1} - n_d}{2}\right), \quad (\text{A.36})$$

where we define

$$\gamma_d \equiv \prod_{\ell=1}^{d-1} \frac{1}{\Gamma(n_\ell/2)} \quad (\text{A.37})$$

as in the main text, as well as the integral function

$$f_q(z; \nu_1, \dots, \nu_q) \equiv \left[\prod_{j=1}^q \int_0^\infty dt_j t_j^{\nu_j - 1} \exp(-t_j) \right] \exp\left(-z \frac{1}{t_1 \cdots t_q}\right) \quad (\text{A.38})$$

for parameters $\nu_j \in \mathbb{R}$ and $z \geq 0$. The claim is that

$$f_q(z; \nu_1, \dots, \nu_q) = G_{0,q+1}^{q+1,0}\left(z \left| \begin{matrix} - \\ 0, \nu_1, \dots, \nu_q \end{matrix} \right.\right), \quad (\text{A.39})$$

which follows directly from the Mellin transform $\mathcal{M}f_q$ of f_q and the definition of the Meijer G -function as the Mellin-Barnes integral (12). For $s \in \mathbb{C}$ such that $\Re(s) > 0$ and $\Re(\nu_j + s) > 0$ for all j , we can easily compute [30]

$$\{\mathcal{M}f_q\}(s; \nu_1, \dots, \nu_q) = \int_0^\infty dz z^{s-1} f_q(z; \nu_1, \dots, \nu_q) = \Gamma(s) \prod_{j=1}^q \Gamma(\nu_j + s). \quad (\text{A.40})$$

For s satisfying the above properties, the properties of the Γ function imply that $\mathcal{M}f_q$ is a function that tends to zero uniformly as $\Im(s) \rightarrow \pm\infty$. Then, by the Mellin inversion theorem [28, 30], we have

$$f_q(z; \nu_1, \dots, \nu_q) = \frac{1}{2\pi i} \int_{c-i\infty}^{c+i\infty} ds z^{-s} \Gamma(s) \prod_{j=1}^q \Gamma(\nu_j + s) \quad (\text{A.41})$$

where the contour is chosen such that $\Re(s) = c$ satisfies the above conditions. This is the definition of the desired Meijer G -function [28, 29], hence we conclude the claimed result.

B Derivation of the prior of a deep ReLU network

In this appendix, we derive the expansion given in §3.3 for the prior of a ReLU network as a mixture of the priors of linear networks of varying widths. Using the linearity of the Fourier transform, the desired result can be stated in terms of characteristic functions as

$$\begin{aligned} \varphi_d^{\text{ReLU}}(\mathbf{q}_d; \kappa_d; n_1, \dots, n_{d-1}) \\ = 1 - \frac{(2^{n_1} - 1)(2^{n_2} - 1) \dots (2^{n_{d-1}} - 1)}{2^{n_1 + \dots + n_{d-1}}} \\ + \frac{1}{2^{n_1 + \dots + n_{d-1}}} \sum_{k_1=1}^{n_1} \dots \sum_{k_{d-1}=1}^{n_{d-1}} \binom{n_1}{k_1} \dots \binom{n_{d-1}}{k_{d-1}} \varphi_d^{\text{lin}}(\mathbf{q}_d; \kappa_d; k_1, \dots, k_{d-1}). \end{aligned} \quad (\text{B.1})$$

We prove this proposition by induction on the depth d .

For a network with a single hidden layer, we can easily evaluate the characteristic function φ_2 for $\phi_1(x) = \max\{0, x\}$ as the integrals factor over the hidden layer dimensions, yielding

$$\varphi_2^{\text{ReLU}}(\mathbf{q}_2) = \left[\frac{1}{2} + \frac{1}{2} (1 + \kappa_2^2 \|\mathbf{q}_2\|^2)^{-1/2} \right]^{n_1}, \quad (\text{B.2})$$

where, as before, $\kappa_2 \equiv \sigma_1 \sigma_2 \|\mathbf{x}\|$. Expanding this result using the binomial theorem, we find that

$$\begin{aligned} \varphi_2^{\text{ReLU}}(\mathbf{q}_2; \kappa_2; n_1) &= \frac{1}{2^{n_1}} \sum_{k=0}^{n_1} \binom{n_1}{k} (1 + \kappa_2^2 \|\mathbf{q}_2\|^2)^{-k/2} \\ &= \frac{1}{2^{n_1}} + \frac{1}{2^{n_1}} \sum_{k=1}^{n_1} \binom{n_1}{k} \varphi_2^{\text{lin}}(\mathbf{q}_2; \kappa_2; k), \end{aligned} \quad (\text{B.3})$$

which proves the base case of the desired result.

We now consider a depth d network. From the definition of the characteristic functions, we have the recursive identity

$$\begin{aligned} \varphi_d^{\text{ReLU}}(\mathbf{q}_d; \kappa_d; n_1, \dots, n_{d-1}) &= \int \frac{d\mathbf{q}_{d-1} d\mathbf{h}_{d-1}}{(2\pi)^{n_{d-1}}} \exp \left(i\mathbf{q}_{d-1} \cdot \mathbf{h}_{d-1} - \frac{1}{2} \sigma_d^2 \|\mathbf{q}_d\|^2 \|\phi(\mathbf{h}_{d-1})\|^2 \right) \\ &\quad \times \varphi_{d-1}^{\text{ReLU}}(\mathbf{q}_{d-1}; \kappa_{d-1}; n_1, \dots, n_{d-2}). \end{aligned} \quad (\text{B.4})$$

By the induction hypothesis, we have

$$\begin{aligned} \varphi_{d-1}^{\text{ReLU}}(\mathbf{q}_{d-1}; \kappa_{d-1}; n_1, \dots, n_{d-2}) \\ = \frac{2^{n_1 + \dots + n_{d-2}} - (2^{n_1} - 1)(2^{n_2} - 1) \dots (2^{n_{d-2}} - 1)}{2^{n_1 + \dots + n_{d-2}}} \\ + \frac{1}{2^{n_1 + \dots + n_{d-2}}} \sum_{k_1=1}^{n_1} \dots \sum_{k_{d-2}=1}^{n_{d-2}} \binom{n_1}{k_1} \dots \binom{n_{d-2}}{k_{d-2}} \varphi_{d-1}^{\text{lin}}(\mathbf{q}_{d-1}; \kappa_{d-1}; k_1, \dots, k_{d-2}). \end{aligned} \quad (\text{B.5})$$

Noting that

$$\int \frac{d\mathbf{q}_{d-1} d\mathbf{h}_{d-1}}{(2\pi)^{n_{d-1}}} \exp \left(i\mathbf{q}_{d-1} \cdot \mathbf{h}_{d-1} - \frac{1}{2} \sigma_d^2 \|\mathbf{q}_d\|^2 \|\phi(\mathbf{h}_{d-1})\|^2 \right) = 1, \quad (\text{B.6})$$

our task is to evaluate the integral

$$\int \frac{d\mathbf{q}_{d-1} d\mathbf{h}_{d-1}}{(2\pi)^{n_{d-1}}} \exp \left(i\mathbf{q}_{d-1} \cdot \mathbf{h}_{d-1} - \frac{1}{2} \sigma_d^2 \|\mathbf{q}_d\|^2 \|\phi(\mathbf{h}_{d-1})\|^2 \right) \varphi_{d-1}^{\text{lin}}(\mathbf{q}_{d-1}; \kappa_{d-1}; k_1, \dots, k_{d-2}). \quad (\text{B.7})$$

By definition,

$$\begin{aligned} \int \frac{d\mathbf{q}_{d-1}}{(2\pi)^{n_{d-1}}} \exp(i\mathbf{q}_{d-1} \cdot \mathbf{h}_{d-1}) \varphi_{d-1}^{\text{lin}}(\mathbf{q}_{d-1}; \kappa_{d-1}; k_1, \dots, k_{d-2}) \\ = p_{d-1}^{\text{lin}}(\mathbf{h}_{d-1}; \kappa_{d-1}; k_1, \dots, k_{d-2}, n_{d-1}), \end{aligned} \quad (\text{B.8})$$

hence the required integral is

$$\int d\mathbf{h}_{d-1} \exp\left(-\frac{1}{2}\sigma_d^2\|\mathbf{q}_d\|^2\|\phi(\mathbf{h}_{d-1})\|^2\right) p_{d-1}^{\text{lin}}(\mathbf{h}_{d-1}; \kappa_{d-1}; k_1, \dots, k_{d-2}, n_{d-1}). \quad (\text{B.9})$$

As p_{d-1}^{lin} is radial, the integral is invariant under permutation of the dimensions of \mathbf{h}_{d-1} . Then, partitioning the domain of integration over \mathbf{h}_2 into regions in which different numbers of ReLUs are active, we have

$$\begin{aligned} & \sum_{k_{d-1}=0}^{n_{d-1}} \binom{n_{d-1}}{k_{d-1}} \int_0^\infty dh_{d-1,1} \cdots \int_0^\infty dh_{d-1,k_{d-1}} \exp\left(-\frac{1}{2}\sigma_d^2\|\mathbf{q}_d\|^2 \sum_{j=1}^{k_{d-1}} h_{d-1,j}^2\right) \\ & \times \int_{-\infty}^0 dh_{d-1,k_{d-1}+1} \cdots \int_{-\infty}^0 dh_{d-1,n_{d-1}} p_{d-1}^{\text{lin}}(\mathbf{h}_{d-1}; \kappa_{d-1}; k_1, \dots, k_{d-2}, n_{d-1}). \end{aligned} \quad (\text{B.10})$$

As the integrand is even in each dimension of \mathbf{h}_{d-1} , we can extend the domain of integration to all of $\mathbb{R}^{n_{d-1}}$ at the expense of a factor of $2^{-n_{d-1}}$:

$$\begin{aligned} & \frac{1}{2^{n_{d-1}}} \sum_{k_{d-1}=0}^{n_{d-1}} \binom{n_{d-1}}{k_{d-1}} \int_{-\infty}^\infty dh_{d-1,1} \cdots \int_{-\infty}^\infty dh_{d-1,k_{d-1}} \exp\left(-\frac{1}{2}\sigma_d^2\|\mathbf{q}_d\|^2 \sum_{j=1}^{k_{d-1}} h_{d-1,j}^2\right) \\ & \times \int_{-\infty}^\infty dh_{d-1,k_{d-1}+1} \cdots \int_{-\infty}^\infty dh_{d-1,n_{d-1}} p_{d-1}^{\text{lin}}(\mathbf{h}_{d-1}; \kappa_{d-1}; k_1, \dots, k_{d-2}, n_{d-1}). \end{aligned} \quad (\text{B.11})$$

We now use the fact that

$$\begin{aligned} & \int_{-\infty}^\infty dh_{d-1,k_{d-1}+1} \cdots \int_{-\infty}^\infty dh_{d-1,n_{d-1}} p_{d-1}^{\text{lin}}(\mathbf{h}_{d-1}; \kappa_{d-1}; k_1, \dots, k_{d-2}, n_{d-1}) \\ & = p_{d-1}^{\text{lin}}(\mathbf{h}_{d-1}; \kappa_{d-1}; k_1, \dots, k_{d-2}, k_{d-1}), \end{aligned} \quad (\text{B.12})$$

which, as noted in the main text, follows from its definition. Next, we note that

$$\begin{aligned} & \int_{-\infty}^\infty dh_{d-1,1} \cdots \int_{-\infty}^\infty dh_{d-1,k_{d-1}} \exp\left(-\frac{1}{2}\sigma_d^2\|\mathbf{q}_d\|^2 \sum_{j=1}^{k_{d-1}} h_{d-1,j}^2\right) \\ & \times p_{d-1}^{\text{lin}}(\mathbf{h}_{d-1}; \kappa_{d-1}; k_1, \dots, k_{d-2}, k_{d-1}) \\ & = \varphi_d^{\text{lin}}(\mathbf{q}_d; \kappa_{d-1}; k_1, \dots, k_{d-1}) \end{aligned} \quad (\text{B.13})$$

by the recursive relationship between the characteristic functions. If $k_{d-1} = 0$, this quantity is replaced by unity. Thus, the integral of interest evaluates to

$$\frac{1}{2^{n_{d-1}}} + \frac{1}{2^{n_{d-1}}} \sum_{k_{d-1}=0}^{n_{d-1}} \binom{n_{d-1}}{k_{d-1}} \varphi_d^{\text{lin}}(\mathbf{q}_d; \kappa_{d-1}; k_1, \dots, k_{d-1}). \quad (\text{B.14})$$

Therefore, after some algebraic simplification of the constant term, we find that

$$\begin{aligned} & \varphi_d(\mathbf{q}_d; \kappa_d; n_1, \dots, n_{d-1}) \\ & = 1 - \frac{(2^{n_1} - 1)(2^{n_2} - 1) \cdots (2^{n_{d-1}} - 1)}{2^{n_1 + \cdots + n_{d-1}}} \\ & + \frac{1}{2^{n_1 + \cdots + n_{d-1}}} \sum_{k_1=1}^{n_1} \cdots \sum_{k_{d-1}=1}^{n_{d-1}} \binom{n_1}{k_1} \cdots \binom{n_{d-1}}{k_{d-1}} \varphi_d^{\text{lin}}(\mathbf{q}_d; \kappa_{d-1}; k_1, \dots, k_{d-1}) \end{aligned} \quad (\text{B.15})$$

under the induction hypothesis, hence we conclude the claimed result.

C Derivation of tail bounds

In this appendix, we use our results for the moments of the preactivation norms to derive the variation of the tail bounds of [21, 22] reported in §4.2. Following the results of Vladimirova et al. [21, 22], it suffices to show that there exist positive constants C_1 and C_2 such that

$$C_1 m^{d/2} \leq (\mathbb{E} \|\mathbf{h}_d\|^m)^{1/m} \leq C_2 m^{d/2} \quad (\text{C.1})$$

for all $m \in \mathbb{N}_{>0}$, holding the widths n_1, \dots, n_d and the depth d fixed. It is of course sufficient to show that $(\mathbb{E} \|\mathbf{h}_d\|^m)^{1/m}$ behaves asymptotically like $m^{d/2}$, as the constants C_1 and C_2 may be chosen small and large enough, respectively, such that this inequality holds for smaller, finite m .

For a linear network, we have (17)

$$(\mathbb{E}_{\text{lin}} \|\mathbf{h}_d\|^m)^{1/m} = 2^{d/2} \kappa_d \prod_{\ell=1}^d \left(\frac{\Gamma[(n_\ell + m)/2]}{\Gamma(n_\ell/2)} \right)^{1/m}. \quad (\text{C.2})$$

By a simple application of Stirling's formula [28], we find that

$$\left(\frac{\Gamma[(n + m)/2]}{\Gamma(n/2)} \right)^{1/m} = \sqrt{\frac{m}{2e}} [1 + \mathcal{O}(m^{-1})] \quad (\text{C.3})$$

as $m \rightarrow \infty$ for any fixed $n \in \mathbb{N}_{>0}$. Therefore, for any finite depth, we conclude the desired result.

For a ReLU network, we have (18)

$$(\mathbb{E}_{\text{ReLU}} \|\mathbf{h}_d\|^m)^{1/m} = 2^{d/2} \kappa_d \left(\frac{\Gamma[(n_d + m)/2]}{\Gamma(n_d/2)} \right)^{1/m} \prod_{\ell=1}^{d-1} \left[\frac{1}{2^{n_\ell}} \sum_{k_\ell=1}^{n_\ell} \binom{n_\ell}{k_\ell} \frac{\Gamma[(k_\ell + m)/2]}{\Gamma(k_\ell/2)} \right]^{1/m}. \quad (\text{C.4})$$

Trivially,

$$\frac{1}{2^n} \sum_{k=1}^n \binom{n}{k} \frac{\Gamma[(k + m)/2]}{\Gamma(k/2)} \leq (1 - 2^n) \frac{\Gamma[(n + m)/2]}{\Gamma(n/2)} \leq \frac{\Gamma[(n + m)/2]}{\Gamma(n/2)}. \quad (\text{C.5})$$

Similarly, we have the trivial lower bound

$$\frac{1}{2^n} \sum_{k=1}^n \binom{n}{k} \frac{\Gamma[(k + m)/2]}{\Gamma(k/2)} \geq (1 - 2^n) \frac{\Gamma[(1 + m)/2]}{\Gamma(1/2)}, \quad (\text{C.6})$$

hence, as $(1 - 2^n)^{1/m} \geq 1/2$ for all $m, n \in \mathbb{N}_{>0}$, we have

$$\frac{1}{2} \left(\frac{\Gamma[(1 + m)/2]}{\Gamma(1/2)} \right)^{1/m} \leq \left(\frac{1}{2^n} \sum_{k=1}^n \binom{n}{k} \frac{\Gamma[(k + m)/2]}{\Gamma(k/2)} \right)^{1/m} \leq \left(\frac{\Gamma[(n + m)/2]}{\Gamma(n/2)} \right)^{1/m}. \quad (\text{C.7})$$

Thus, by virtue of the above result for linear networks, we obtain the desired result.

D Derivation of the asymptotic prior distribution at large widths

In this appendix, we derive the asymptotic behavior of the prior distribution for large hidden layer widths reported in §4.3. We first consider linear networks. We assume the parameterization described in the main text, which yields

$$\mathbb{E} h_i h_j = \varkappa_d^2 \delta_{ij} \quad (\text{D.1})$$

for \varkappa_d independent of width. Then, using the fact that all odd-ordered cumulants of the zero-mean random vector \mathbf{h}_d vanish, the third-order Edgeworth approximation to the prior is

$$\begin{aligned} p_d(\mathbf{h}_d | \mathbf{x}) &\approx \frac{1}{(2\pi \varkappa_d^2)^{n_d/2}} \exp \left(-\frac{\|\mathbf{h}_d\|^2}{2\varkappa_d^2} \right) \\ &\times \left[1 + \frac{1}{24} \chi_{ijkl} \left(\frac{1}{\varkappa_d^8} h_i h_j h_k h_l - \frac{6}{\varkappa_d^6} \delta_{kl} h_i h_j + \frac{3}{\varkappa_d^2} \delta_{ij} \delta_{kl} \right) \right], \end{aligned} \quad (\text{D.2})$$

where

$$\chi_{ijkl} = \mathbb{E}h_i h_j h_k h_l - \mathbb{E}(h_i h_j)\mathbb{E}(h_k h_l) - \mathbb{E}(h_i h_k)\mathbb{E}(h_j h_l) - \mathbb{E}(h_i h_l)\mathbb{E}(h_j h_k) \quad (\text{D.3})$$

is the fourth joint cumulant and summation over repeated indices is implied [37]. For this Edgeworth approximation to yield an asymptotic approximation to the prior (i.e., for higher terms to be suppressed in the limit of large widths), the sixth and higher cumulants of \mathbf{h}_d must be suppressed relative to the fourth cumulant. However, using the radial symmetry of the distribution and the moments (17), we can see that these cumulants will be of $\mathcal{O}(n^{-2})$.

We now note that the only non-vanishing terms will be those of the form χ_{iiii} , χ_{iijj} , χ_{ijij} , or χ_{jiij} , and that

$$\chi_{iiii} = \mathbb{E}h_i^4 - 3(\mathbb{E}h_i^2)^2, \quad (\text{D.4})$$

while

$$\chi_{iijj} = \chi_{ijij} = \chi_{jiij} = \mathbb{E}h_i^2 h_j^2 - \mathbb{E}(h_i^2)\mathbb{E}(h_j^2). \quad (\text{D.5})$$

By symmetry or by direct calculation in spherical coordinates, we have

$$\mathbb{E}h_1^4 = 3\mathbb{E}h_1^2 h_2^2 = 3\kappa_d^4 \prod_{\ell=1}^{d-1} [n_\ell(n_\ell + 2)] = 3\kappa_d^4 \prod_{\ell=1}^{d-1} \frac{n_\ell + 2}{n_\ell}, \quad (\text{D.6})$$

hence

$$\chi_{iiii} = 3\chi_{iijj} = 3\kappa_d^4 \left[\prod_{\ell=1}^{d-1} \frac{n_\ell + 2}{n_\ell} - 1 \right]. \quad (\text{D.7})$$

Therefore, approximating χ_{iiii} to $\mathcal{O}(n^{-1})$, we obtain the following third-order Edgeworth approximation for the prior density:

$$\begin{aligned} p_d(\mathbf{h}_d | \mathbf{x}) &\approx \frac{1}{(2\pi\kappa_d^2)^{n_d/2}} \exp\left(-\frac{\|\mathbf{h}_d\|^2}{2\kappa_d^2}\right) \\ &\times \left[1 + \frac{1}{4} \left(\sum_{\ell=1}^{d-1} \frac{1}{n_\ell} \right) \left(\frac{\|\mathbf{h}_d\|^4}{\kappa_d^4} - 2(n_d + 2) \frac{\|\mathbf{h}_d\|^2}{\kappa_d^2} + n_d(n_d + 2) \right) + \mathcal{O}\left(\frac{1}{n^2}\right) \right]. \end{aligned} \quad (\text{D.8})$$

Upon integration, the second term inside the square brackets vanishes, hence this approximate density is properly normalized.

For ReLU networks, the story is much the same, except we now have $\mathbb{E}h_i h_j = 2^{1-d} \kappa_d^2 \delta_{ij}$ and

$$\mathbb{E}h_1^4 = 3\mathbb{E}h_1^2 h_2^2 = 3 \times 4^{1-d} \kappa_d^4 \prod_{\ell=1}^{d-1} [n_\ell(n_\ell + 5)] = 3 \times 4^{1-d} \kappa_d^4 \prod_{\ell=1}^{d-1} \frac{n_\ell + 5}{n_\ell}, \quad (\text{D.9})$$

hence we conclude that

$$\begin{aligned} p_d^{\text{ReLU}}(\mathbf{h}_d | \mathbf{x}) &\approx \frac{1}{(2^{2-d}\pi\kappa_d^2)^{n_d/2}} \exp\left(-\frac{\|\mathbf{h}_d\|^2}{2^{2-d}\kappa_d^2}\right) \\ &\times \left[1 + \frac{5}{4} \left(\sum_{\ell=1}^{d-1} \frac{1}{n_\ell} \right) \left(\frac{\|\mathbf{h}_d\|^4}{4^{1-d}\kappa_d^4} - 2(n_d + 2) \frac{\|\mathbf{h}_d\|^2}{2^{1-d}\kappa_d^2} + n_d(n_d + 2) \right) \right. \\ &\quad \left. + \mathcal{O}\left(\frac{1}{n^2}\right) \right]. \end{aligned} \quad (\text{D.10})$$

One can immediately see that these approximate distributions are sub-Gaussian. To show this more formally, we note that the moments of the approximate distribution for a linear network are

$$(\mathbb{E}_{\text{EW}} \|\mathbf{h}_d\|^m)^{1/m} = \sqrt{2}\kappa_d \left(\frac{\Gamma[(n_d + m)/2]}{\Gamma(n_d/2)} \right)^{1/m} \left[1 + \frac{1}{4} \left(\prod_{\ell=1}^{d-1} \frac{1}{n_\ell} \right) m(m-2) \right]^{1/m}. \quad (\text{D.11})$$

For all $m \geq 2$ and $0 \leq t \leq 1$, we have

$$1 \leq [1 + m(m-2)t]^{1/m} \leq (m-1)^{2/m} \leq 2, \quad (\text{D.12})$$

where the upper bound is sub-optimal but sufficient for our purposes. Then, we conclude that

$$\sqrt{2}\varkappa_d \left(\frac{\Gamma[(n_d+m)/2]}{\Gamma(n_d/2)} \right)^{1/m} \leq (\mathbb{E}_{\text{EW}} \|\mathbf{h}_d\|^m)^{1/m} \leq 2\sqrt{2}\varkappa_d \left(\frac{\Gamma[(n_d+m)/2]}{\Gamma(n_d/2)} \right)^{1/m} \quad (\text{D.13})$$

for all $m \geq 2$. Moreover, we can easily see that similar bounds will hold for the approximation to the prior of a ReLU network, up to overall factors scaling \varkappa_d . Therefore, applying the results of Appendix C, we conclude that these approximations are sub-Weibull with optimal tail exponent $1/2$, implying that they are sub-Gaussian.

E Numerical methods

Here, we summarize the numerical methods used to generate Figures 1, 2, 3, and 4. All computations were performed using **MATLAB** versions 9.5 (R2018b) and 9.8 (R2020a).¹ The theoretical prior densities were computed using the `meijerG` function, and evaluated with variable-precision arithmetic. Empirical distributions were estimated with simple Monte Carlo sampling: for each sample, the weight matrices were drawn from isotropic Gaussian distributions, and then the output preactivation was computed. In these simulations, the input was taken to be one-dimensional and to have a value of unity. Furthermore, we fixed $\kappa_d^2 = (n_1 \cdots n_{d-1})^{-1}$ for linear networks and $\kappa_d^2 = 2^{d-1}(n_1 \cdots n_{d-1})^{-1}$ for ReLU networks, such that the output preactivations had identical variances.

The computations required to evaluate the theoretical priors and sampling-based estimates in Figures 1 and 3 were performed across 32 CPU cores of one node of Harvard University’s Cannon HPC cluster.² The computational cost of our work was entirely dominated by evaluation of the theoretical ReLU network prior. To reduce the amount of computation required to evaluate the ReLU network prior at large widths, we approximated the full mixture (16) by neglecting terms with weighting coefficients $2^{-n_\ell \binom{n_\ell}{k_\ell}}$ less than the floating-point relative accuracy $\text{eps} = 2^{-52}$. More precisely, our code evaluates the logarithm of the weighting coefficient using the $\log \Gamma$ function (`gamma1n` in **MATLAB**) for numerical stability, and then compares the logarithms of these two non-negative floating point values. This cutoff only truncates the sum for networks of width $n = 100$ at depths $d = 2, 3$, and 4 ; the full mixture is evaluated for narrower networks. For $n = 100$, it reduces the number of summands from 10^2 , 10^4 , and 10^6 to 77, 4,537, and 208,243, respectively. We have confirmed that the resulting approximation to the exact prior behaves monotonically with respect to the cutoff for values larger than `eps`. With this cutoff, 24 seconds, 3.5 hours, and 153 hours of compute time were required to compute the theoretical prior for these depths, respectively. In all, we required just under 160 hours of compute time to produce the figures shown here.

¹Our code is available at <https://github.com/Pehlevan-Group/ExactBayesianNetworkPriors>.

²See <https://www.rc.fas.harvard.edu/about/cluster-architecture/> for details.